8.1 Introduction

Nickel, is the fifth most abundant element found ubiquitously in the biosphere by being a common component of natural and fresh waters due to erosion and weathering. The presence of Ni(II) in waste-water discharges is frequent as it is extensively employed in a number of industries including electroplating, battery and accumulator manufacturing, mining and metallurgical processing, leather tanning, wood preservation, fossil fuel combustion and waste incineration, pulp processing, tableware plating, dye house effluent, paint and ink formulation, porcelain enamelling activities, etc. Besides, discharges from steel works, motor vehicle and aircraft industries, and printing are potential sources of nickel [Patterson, 1985] contamination to water sources. Silver refineries are reported to discharge high levels of nickel in aquatic sources. The high consumption of nickel-containing products inescapably leads to environmental pollution by nickel and its by-products at all stages of production, recycling and disposal. In waste streams, Nickel is known to exist predominantly as the soluble ion which may get change into stable form in presence of complexing agents such as ammonia, EDTA, or cyanide. The formation of such stable nickel–cyanide complexes interpose with both cyanide and nickel treatment leading to high levels of both cyanide and nickel in treated wastewater effluents. Among Ni (IV) and Ni (II), the latter is a more toxic and carcinogenic form of the metal. According to World Health Organization (WHO), exposure to nickel compounds above the permissible limit of 0.1 mg/L in drinking water can have adverse

effects on human health [Pane et al., 2003; Denkhaus and Salnikow, 2002; Can et al., 2006; Oladipo and Gazi, 2015]. The US Environmental Protection Agency (EPA) has fixed its maximum permissible concentration in drinking water to be 0.5 mg/L [Gupta et al., 2010].

In contrast to other metals, nickel ion is more intractable, the higher concentration of which in ingested water may cause severe damage to lungs, kidneys, gastrointestinal distress, e.g., nausea, vomiting, diarrhea, pulmonary fibrosis, renal edema, and skin dermatitis [Akhtar et al., 2004; Garg et al., 2008]. This is due to its toxic effects on living systems so that stringent limits have been stipulated for discharge of Ni (II) into the environment and removal of Nickel from water and wastewaters has become imperative.

Various conventional methods, namely chemical precipitation, ion exchange, membrane processes, flotation, electrochemical treatment coagulation, flocculation and adsorption were designed to remove heavy metals from wastewater [Ku and Jung, 2001; Kang et al., 2004; Landaburu-Aguirre et al., 2009; Lundh et al., 2000; Wang et al., 2007; El Samrani et al., 2008] were designed. Adsorption process is commonly employed because of its performance, ease of operation, the possible use of renewable and biodegradable adsorbents, low energy requirements, capacity to treat very dilute wastewater, recony and recycling of the adsorbent, and recony of heavy metals, as well as its cost effectiveness [Volesky, 2004; Ozcan and Ozcan, 2013; Kamari et al., 2009]. In the past few decades, nano-technology has revolutionized almost every branch of science and technology and nanomaterials have been extensively explored for various applications including water treatment. Among several nanoparticles, Cupric oxide (CuO)

nanoparticles are of momentous technological interest and have attracted more attention due to their unique properties. Cupric oxide forms the basis of high-temperature superconductors, gas sensors, extensively employed as an anti-biotic, anti-fungal and anti-microbial agent when incorporated in coatings, plastics and textiles, as pesticides in pesticide formulations [Zhang et al., 2014]. In water treatment, nano-scaled CuO has been efficiently used for removal of As(III) and As(VI) [Carol et al., 2009].

The current study deals with the investigation of adsorptive potential of CuO nanoparticles for adsorption of Ni (II) ions from aqueous solutions. The combined effects of pH, Ni (II) ion concentration and adsorbent dosage on the adsorption process were investigated by Box-Behnken design (BBD) of experimental design in response surface methodology (RSM). The isotherm, kinetic and thermodynamic parameters were evaluated for the adsorption process. Linear and non-linear analyses of isotherm and kinetic parameters was carried out and compared for obtaining the best fit parameters.

8.2 Results and discussions

8.2.1 Characterization of nano-cupric oxide

The detailed study on the structural and topographical characterization of Cupric oxide nanoparticles before adsorption has been presented in Section 4.3.3 of Chapter 4. The X-ray diffraction pattern of nano-cupric oxide after adsorption of nickel displayed no additional peak suggesting structural changes did not occur during the process (Figure 8.1). In the same way, absence of extra peak in the FTIR after adsorption suggested that the process of removal was physical in nature (Figure 8.2).
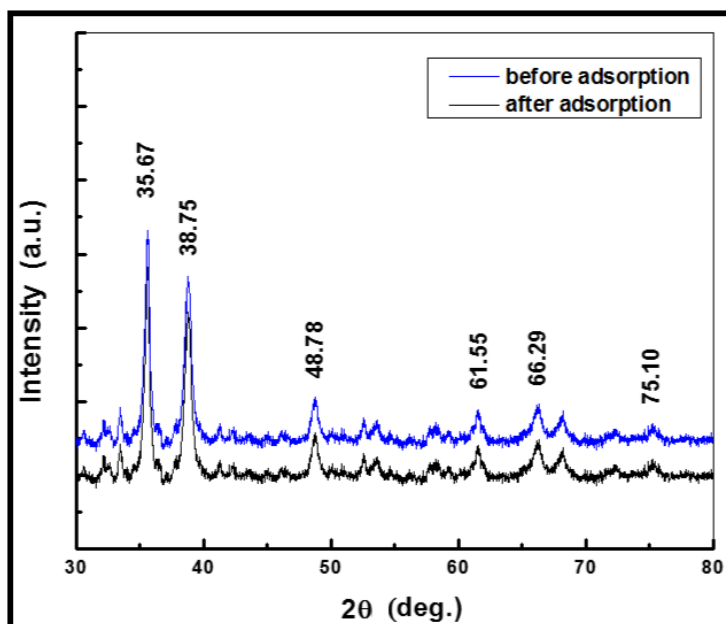
Figure 8.1 XRD pattern of nano-cupric oxide before and after adsorption of Ni(II) ions
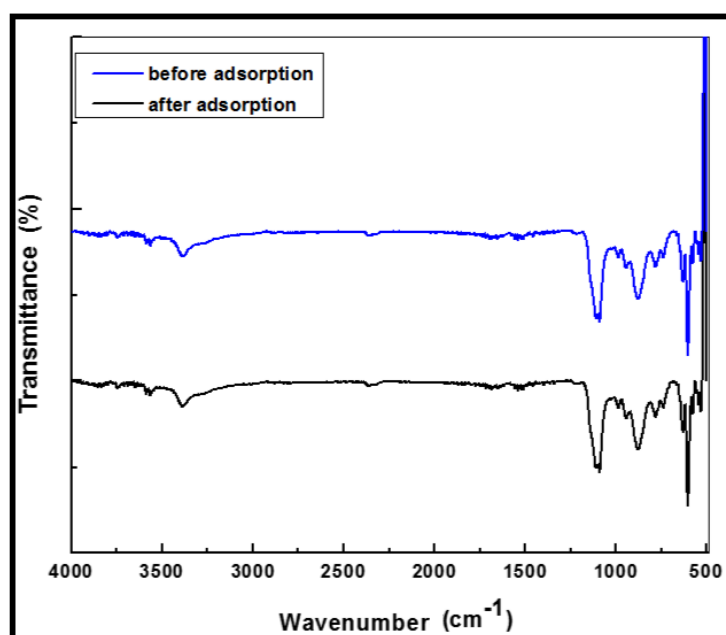

Figure 8.2 FT-IR spectrum of nano-cupric oxide before and after adsorption of Ni(II) ions

Elemental composition was also explored after adsorption through EDS and the spectrum revealed peaks of Ni along with the peaks of Cu and O that confirmed its adherence on the surface (Figure 8.3).
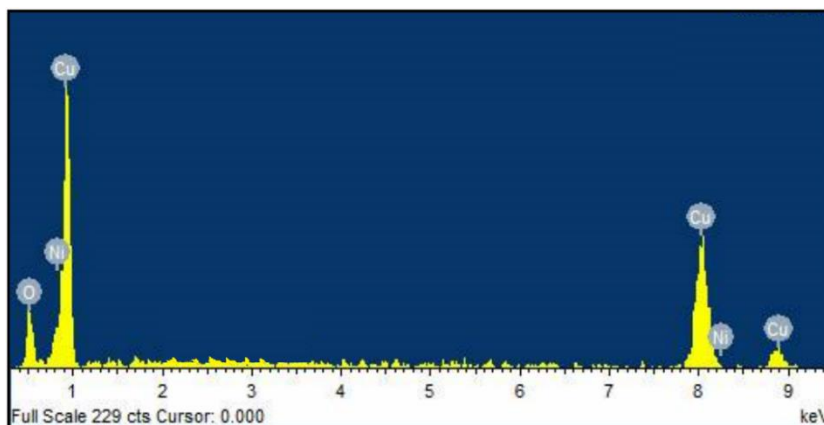

Figure 8.3 EDS pattern of nano-cupric oxide after adsorption

8.2.2 Adsorption Experiments

The experiments were carried out in batch mode for the adsorption study of Ni ions on nano-cupric oxide.

8.2.2.1 Effect of experimental parameters on the removal of nickel from aqueous solution

Investigation of impact of various parameters namely pH, adsorbent dose and initial metal ion concentration was carried out through preliminary experiments and the results revealed that acidic conditions decreased the adsorption while increasing pH showed augmentation of removal. The percentage of Ni(II) adsorbed by Cupric oxide nanoparticles was increased when the pH of the solution was augmented from 2.0 to 7.5

(Figure 8.4). The optimal removal of Ni in the present system was achieved at pH 7.0, and hence this pH was selected for the rest of the experiments. Similarly, adsorption of nickel enhanced with increased dosage of adsorbent keeping other experimental conditions incessant as shown in Figure 8.5. The influence of initial metal concentration was investigated by conducting experiments with different initial Ni(II) concentrations ranging from 15 mg/L to 35 mg/L. At lower metal ion concentration, due to high ratio of available free sites on the adsorbent surface and metal ions in solution, the removal percentage is higher for lower concentration and vice versa as shown in Figure 8.6. It was found that removal declined on raising concentration from 15 mg/L to 35 mg/L.
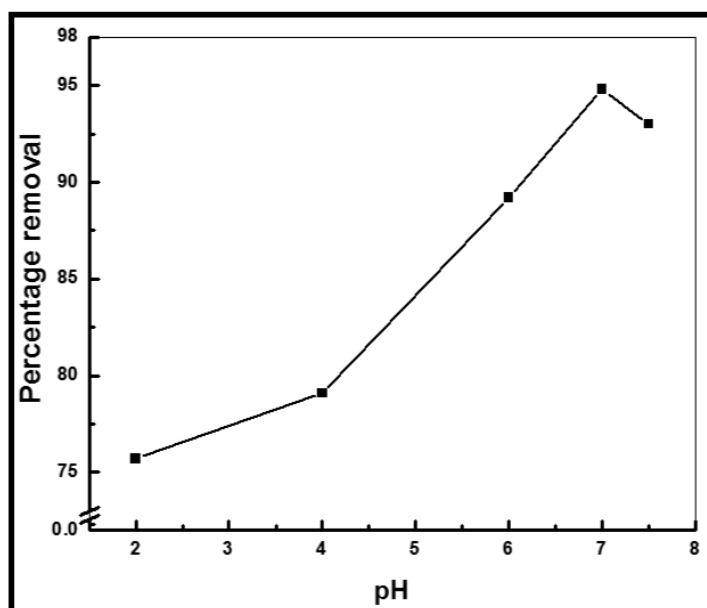

Figure 8.4 Effect of initial pH on removal (%) of nickel from aqueous solution on nano-cupric oxide (Initial concentration= 20 mg/L, adsorbent dose=6 g/L, Temperature= 303K)

The contact time of the system was evaluated by conducting experiment with 20 mg/L of nickel solution at pH 7.0 and adsorbent dose of 6g/L for different time intervals. It was observed that the adsorption rate for metal ion increases in the beginning and after 30 min the adsorption rate become roughly steady and finally adsorption equilibrium was achieved within 30 min (Figure 8.7). After 30 min, there were no significant changes marked in the removal of metal ions.
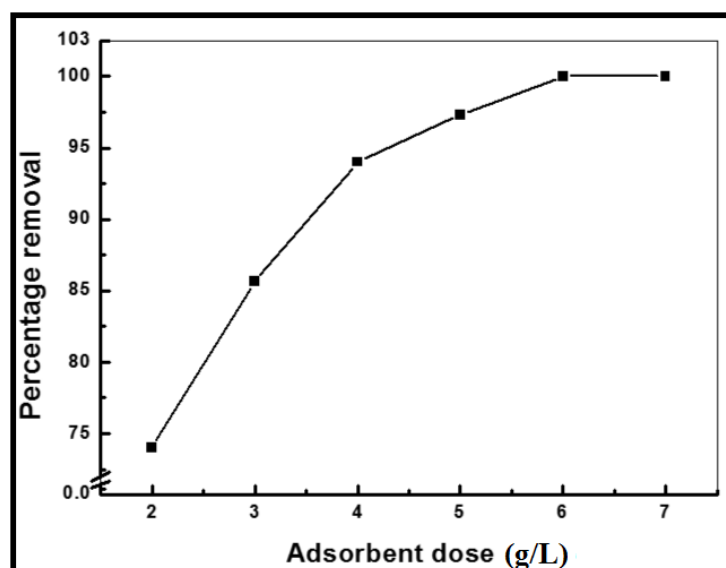

Figure 8.5 Effect of adsorbent dose on removal (%) of nickel from aqueous solution on nano-cupric oxide (Initial pH=7.0, Initial concentration=20mg/L, Temperature 303K)
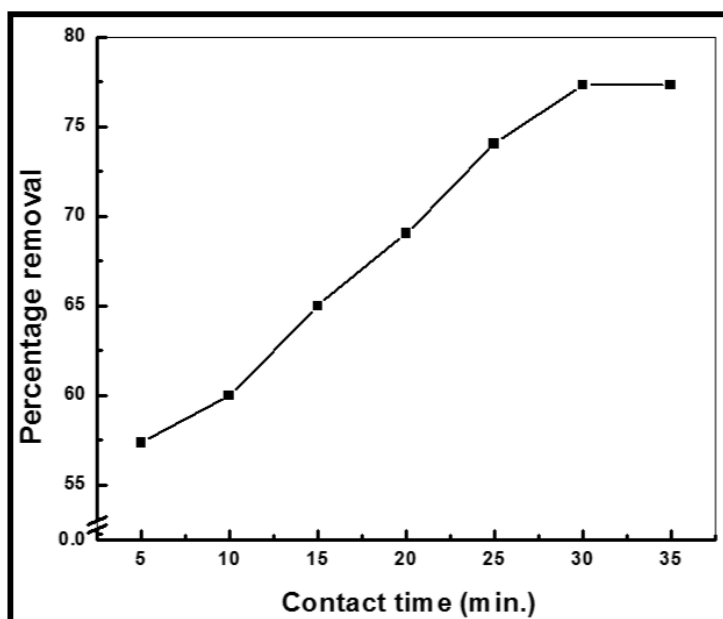
Figure 8.6 Effect of contact time on removal (%) of nickel from aqueous solution on nano-cupric oxide (Initial concentration=20mg/L, Initial pH =7, Initial dose=6g/L, Temperature= 303K)
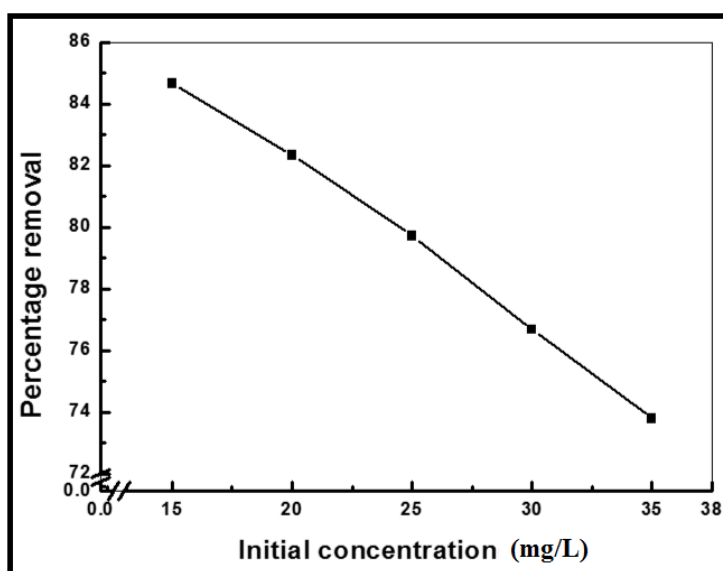

Figure 8.7 Effect of initial concentration on removal (%) of nickel from aqueous solution on nano-cupric oxide (Initial pH= 7, Initial dose=6g/L, Temperature=303 K)

8.2.2.2 Design of experiment and data analysis for adsorption of Nickel (II) on nano-cupric oxide

The adsorption experiments were conducted based on the design matrix of Box-Behnken design of RSM for obtaining the response corresponding to the independent variables addressed in the experimental design matrix by applying quadratic model and corresponding results obtained have been presented in Table 8.1.

Table 8.1 Box-Behnken designed experimental runs for removal of nickel on nano-cupric oxide

Run Order	Concentration (mg/L)	pH	Dose (g/L)	Percent removal
1	5	2	11	55.22
2	25	2	11	73.39
3	5	7	11	100
4	25	7	11	97.52
5	5	4.5	2	86.48
6	25	4.5	2	89.31
7	5	4.5	20	100
8	25	4.5	20	100
9	15	2	2	47.3
10	15	7	2	74.28
11	15	2	20	57.03
12	15	7	20	100
13	15	4.5	11	90.03
14	15	4.5	11	91.23
15	15	4.5	11	90.63

On the basis of experimental findings, the empirical relationship between the response and the independent variables namely initial concentration, pH and adsorbent dose in the coded units is presented in the form of following polynomial regression equation for removal (%) of nickel designated by Y:

$Y = 90.6300 -2.3150$ *(concentration)* $+ 17.3575$ *(pH)* $+ 7.4575$ *(adsorbent dose)* $+ 7.5987$ *(concentration)^2* $- 16.6963$ *(pH)^2* $- 4.2812$ *(adsorbent dose)^2* $- 5.1625$ *(concentration x pH)* $- 0.7075$ *(concentration x adsorbent dose)* $+ 3.9975$ *(pH x adsorbent dose)*.   (8.1)

The hierarchical nature of this model was supported by maintaining the insignificant terms in this study and has been included in the given regression equation [Dahlan et al., 2008]. In the quadratic equation (Equation 8.1), the magnitude of the coefficient represents the intensity while the sign before the coefficient designates nature of influence (positive or negative) of the particular variable on the response. A positive sign of a factor means that the response is upgraded when the factor level augments and a negative effect of the factor revealed that the response is suppressed with the increase in factor level. Upon regression analysis, the regression equation for removal of nickel with Cupric oxide nanoparticles yielded regression coefficient $R^2 = 99.17$, higher than the R^2 (adj.) $= 97.67$ (Table 8.2) that endorses the process of adsorption in the given range of experimental conditions.

The parameters bearing positive sign before their corresponding coefficients inclined to increase the nickel removal (%) and vice versa [Sarkar and Majumdar, 2011]. From the equation, it has been deciphered that pH is the most dominating parameter having positive sign before its coefficient followed by adsorbent dose and concentration. Positive sign before coefficients of both pH and concentration suggested the increment in nickel removal (%) with increase in pH and concentration.

Table. 8.2 Estimated regression coefficients for removal of nickel on nano-cupric oxide

Term	Coef	SE Coef	T	P
Constant	90.63	1.5773	57.458	0
Concentration	2.315	0.9659	2.397	0.062
pH	17.3575	0.9659	17.97	0
Dose	7.4575	0.9659	7.721	0.001
Conc*Conc	7.5987	1.4218	5.344	0.003
pH*pH	-16.6963	1.4218	-11.743	0
Dose*Dose	-4.2812	1.4218	-3.011	0.03
Conc*pH	-5.1625	1.366	-3.779	0.013
Conc*Dose	-0.7075	1.366	-0.518	0.627
pH*Dose	3.9975	1.366	2.926	0.033
S = 2.73203		**PRESS=587.218**		
R-Sq=99.17%		**R-Sq(pred)=86.89%**	**R-Sq(adj)= 97.67%**	

8.2.2.3 Analysis of variance (ANOVA)

The efficacy of the model was investigated by applying analysis of variance (ANOVA) and the results were presented in Table 8.3.

Table 8.3 Analysis of variance for removal of nickel on nano-cupric oxide

Source	DF	Seq SS	Adj SS	Adj MS	F	P
Regression	9	4442.19	4442.19	493.58	66.13	0
Linear	3	2898.05	2898.05	966.02	129.42	0
Concentration	1	42.87	42.87	42.87	5.74	0.062
pH	1	2410.26	2410.26	2410.26	322.92	0
Dose	1	444.91	444.91	444.91	59.61	0.001
Square	3	1371.61	1371.61	457.2	61.25	0
Concentration*Concentration	1	308.96	213.2	213.2	28.56	0.003
pH* pH	1	994.97	1029.29	1029.29	137.9	0
Dose*Dose	1	67.68	67.68	67.68	9.07	0.03
Interaction	3	172.53	172.53	57.51	7.7	0.025
Concentration*pH	1	106.61	106.61	106.61	14.28	0.013
Concentration*Dose	1	2	2	2	0.27	0.627
pH*Dose	1	63.92	63.92	63.92	8.56	0.033
Residual Error	5	37.32	37.32	7.46		
Lack-of-Fit	3	36.6	36.6	12.2	33.89	0.029
Pure Error	2	0.72	0.72	0.36		
Total	14	4479.51				

In present case, ANOVA study exhibited that the regression model is significant as large F-value and a low P value [Jain et al., 2011]. Among linear effect, pH was found to be the dominant parameter among other having sum of squares (Seq SS) value of 2410.26 followed by adsorbent dose and concentration. Similarly, among square effect, pH*pH was dominant and among interactive effect concentration*pH was significant on the basis of sum of squares value.

8.2.2.4 Interaction effect of initial Ni(II) concentration and adsorbent dose

The adsorption experiments based on the matrix predicted by the selected model were conducted with the scheduled concentration range and the desired adsorbent dosage to evaluate their combined effect on the percent removal of nickel ions from the aqueous solutions. From the regression equations, it is evident that coefficient of concentration is having negative sign that indicates decline in percent removal with escalation in the concentration of solution (Runs 6 and 7; Runs 10 and 12). This behavior can be attributed to the lesser availability of active sites available on the adsorbent surface due to saturation for interaction with ions present in solution with increase in the concentration of solution [Sharma and Srivastava, 2010, Wang, 2011]. The graphical representation of the interactions of the result of experimentation has been presented in the form of contour and surface plots as shown in Figure 8.7a and 8.7b Contour plots and surface plots provide assistance in understanding the relationship between the response and experimental levels of each variable under investigation. Both these plots revealed that

removal percent of Ni(II) decreased on increment in initial metal ion concentration and increased with the increase in adsorbent dose.
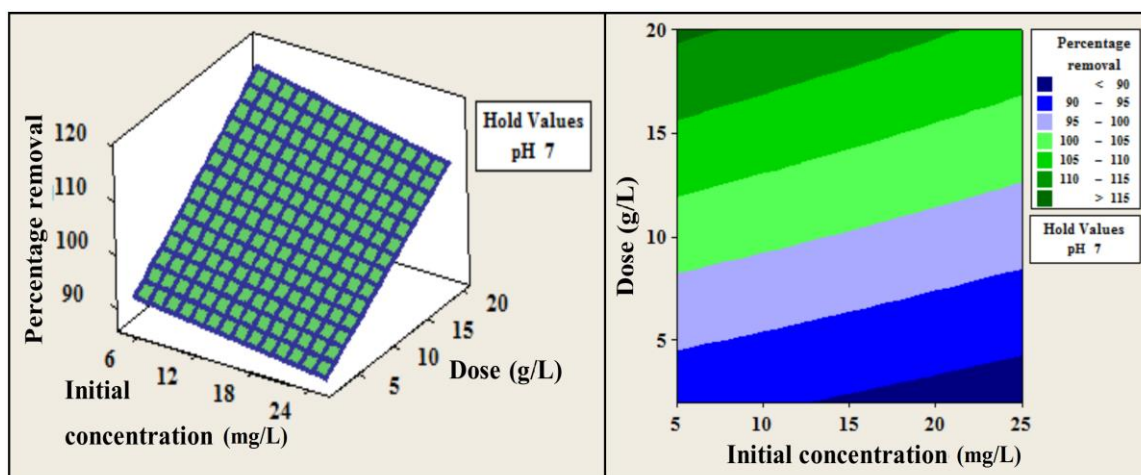

Figure 8.8 (a) Surface plot; and (b) Contour plot of percentage removal vs. dose and concentration at hold value of pH at 7

8.2.2.5 Interaction effect of pH and adsorbent dose

pH is acknowledged as one of the most important parameters in any adsorption processes. It is reported that variation in pH of solution significantly affects the surface of the adsorbent and degree of ionization in solution. Perusal on literature suggested that depending on the pH of the solution different species of metal ions are present in the solution along with the adsorbate and their removal is greatly influenced by the type of their species present in the system at any particular pH.

The speciation diagram of nickel depicted that Ni^{2+} is the only important oxidation state in its aqueous chemistry up to pH 8.0. The interactive effect of both these variables viz., pH and adsorbent dose upon adsorption is shown in Figure 8.9a and 8.9b. It has been

observed that optimum removal is achieved at higher pH and higher dose, as displayed in (Runs 3 and 5; Runs 9 and 12). Both these variables collectively depicted that increased number of positive species and surface active sites held responsible for increased percent removal of adsorbate ions [Davarnejad et al., 2015; Reddy et al., 2011].
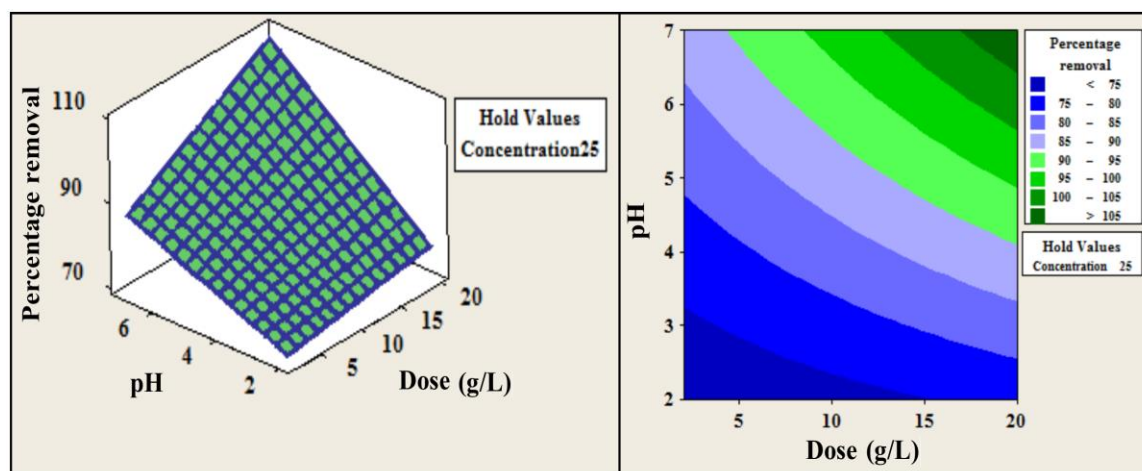

Figure 8.9. (a) Surface plot; and (b) Contour plot of percentage removal vs. pH and dose at hold value of concentration at 25 mg/L

8.2.2.6 Interaction effect of pH and initial Ni(II) concentration

Figure 8.10a and 8.10b displayed the interactive effect of pH and initial metal ion concentration on the percent removal of Ni(II). It has been displayed by (Runs "2 and 5") and (Runs "9 and 12") that increasing initial concentration and varying pH of the solution by keeping dose at a constant value, removal percent decreases gradually. This might be due to the greater ratio of available surface for adsorbate ions at low concentration whereas at higher concentration this ratio decreases thereby tending to decline the overall

removal of adsorbate ions from solutions [Davarnejad et al., 2015; Saadat and Jashni, 2011].
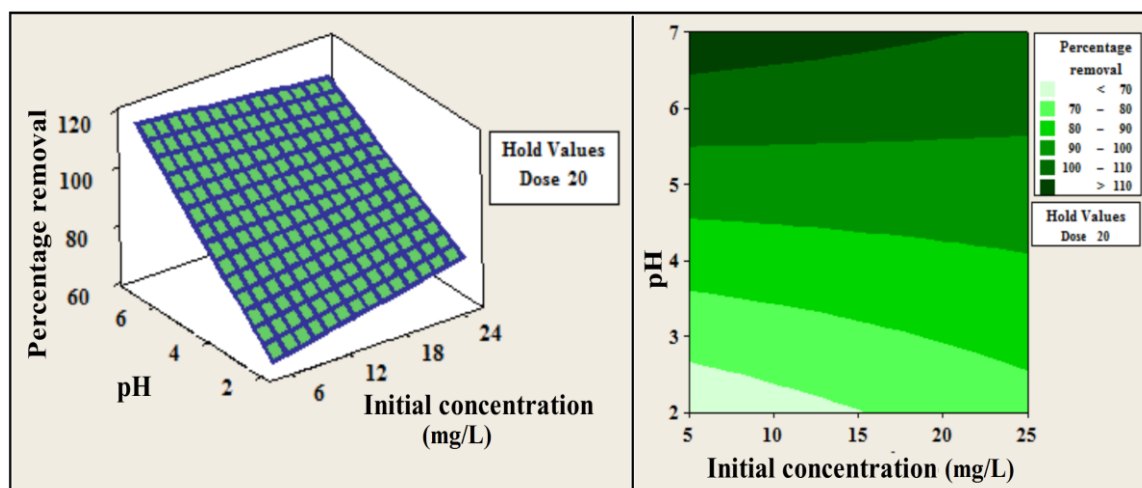

Figure 8.10 (a) Surface plot; and (b) Contour plot of percentage removal vs. pH and concentration at hold value of dose at 20 g/L

8.2.2.7 Interpretation of process optimization of removal (%) of nickel on nano-cupric oxide

The optimum value for desired response was predicted by response optimization plot Figure 8.11. It predicted the optimum value for 100% removal of Ni(II) from aqueous solutions via the process of adsorption on Cupric oxide nanoparticles for the given model (pH 5.8, initial concentration 25mg/L, adsorbent dose 18.8 g/L) with the desirability score 0.9959. In order to verify the efficacy of model, confirmatory experiments were conducted at the predefined conditions. Further, for the confirmation experiment dose and pH were rounded off to 19g/L and 6, respectively and the experimental results were analyzed.
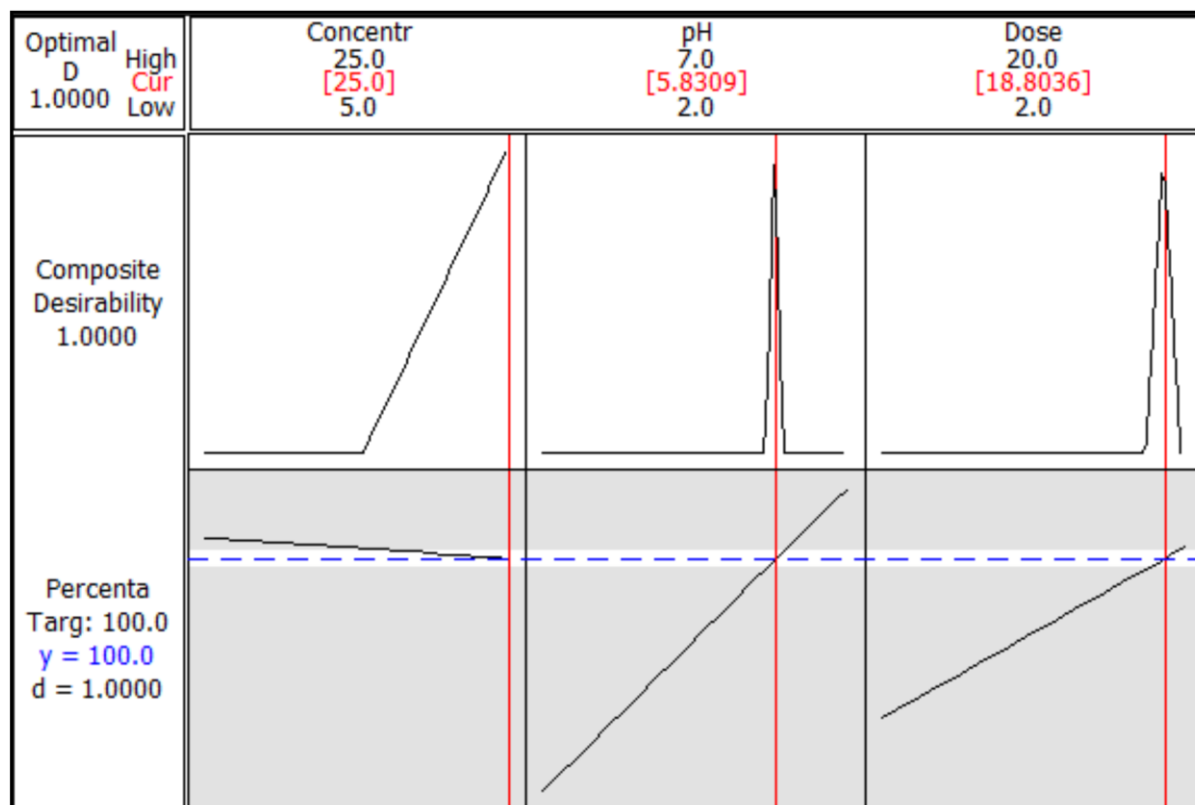
Figure 8.11. Response optimization plot for nickel removal on nano-cupric oxide

However, results showed certain degree of variation than that of predicted by model. The experimental values of the model together with the percentage error difference between the experimental and predicted value has been tabulated in Table 8.4.

Table 8.4 Confirmation experiments for removal of Nickel on nano-cupric oxide

S. No.	Concentration (mg/L)	pH	Dose (g/L)	Experimental values (%)	Predicted values (%)
1	15	7	6.0	96.66	94.48
2	20	7	6.0	92.55	93.26
3	25	7	4.0	90.40	92.03
4	25	6	19.0	89.68	100.0

8.2.3 Adsorption isotherm study

In the present study, the equilibrium data incurred for Ni(II) removal was examined with two parameters isotherms viz. Langmuir and Freundlich to ascertain the most desirable one. Additionally, linear and non-linear analyses were performed for achieving the best fit isotherm model. The following linear and non-linear equations of Langmuir and isotherm model were used [Sharma et al., 2008; Langmuir, 1916]:

$$C_e/q_e = 1/Q^o b + C_e/Q \qquad (8.2)$$

$$q_e = bQ^o C_e/1 + bC_e \qquad (8.3)$$

where, C_e (mg/l) is the equilibrium concentration of the solute, q_e (mg/g) is amount adsorbed at equilibrium and Q^0 (mg/g) and b (L/mg) are constants related to the adsorption capacity and energy of adsorption, respectively.

Freundlich isotherm model was fitted through following linear and non-linear equations [Freundlich, 1906; Allen and McKay, 1980]:

$$log\ q_e = log\ K_F + 1/n\ log\ C_e \tag{8.4}$$

$$q_e = K_F\ C_e^{1/n} \tag{8.5}$$

where, K_F and n are the Freundlich constants. Here, n giving a sign of how congruous the adsorption process is, and K_F $(mg/g(L/mg)^{1/n})$ represents the quantity of metal ion adsorbed on the adsorbent for a unit equilibrium concentration.

8.2.3.1 Linear analysis of adsorption isotherm

The equilibrium data obtained has been fitted to linear equations of Langmuir and Freundlich adsorption isotherm models. The values of theoretical maximum adsorption capacity, Q^0 $(mg\ g^{-1})$ and Langmuir adsorption constant b $(L\ mg^{-1})$ were obtained from the slope and intercept of the plot of C_e/q_e vs. C_e, respectively (Figure 8.12) and the parameters of Freundlich isotherm model such as the capacity, K_F (mg/g) and intensity, n $(g\ L^{-1})$ of the adsorption were calculated from the intercept and slope of the linear plot of ln qe vs. ln C_e, respectively as shown in Figure 8.13. K_F value as well as n showed increment with increase in temperature affirmed the endothermic nature of removal process. The fitness of experimental data was evaluated at different temperatures. The constant parameters and correlation coefficients (R^2) obtained from the plots of known equation for Langmuir and Freundlich have been summarized in Table 8.5. The high correlation coefficient at all temperatures exhibited that Langmuir model provides the

best correlation and thus applicable for interpretation of the experimental data on the
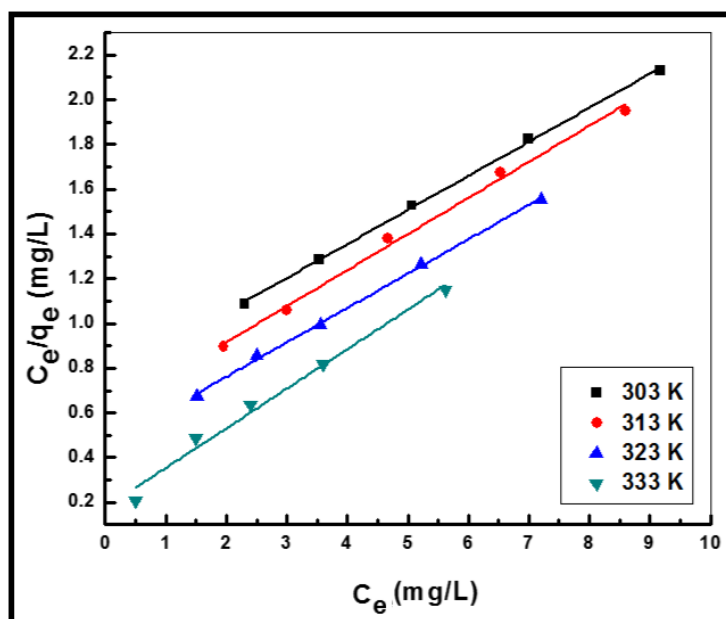
whole concentration range.

Figure 8.12 Linear Langmuir isotherm plot of nickel removal on nano-cupric oxide (symbols represent the experimental data and straight lines represent the data estimated by the model)

Figure 8.13 Linear Freundlich isotherm plot of nickel removal on nano-cupric oxide (symbols represent the experimental data and straight lines represent the data estimated by the model)
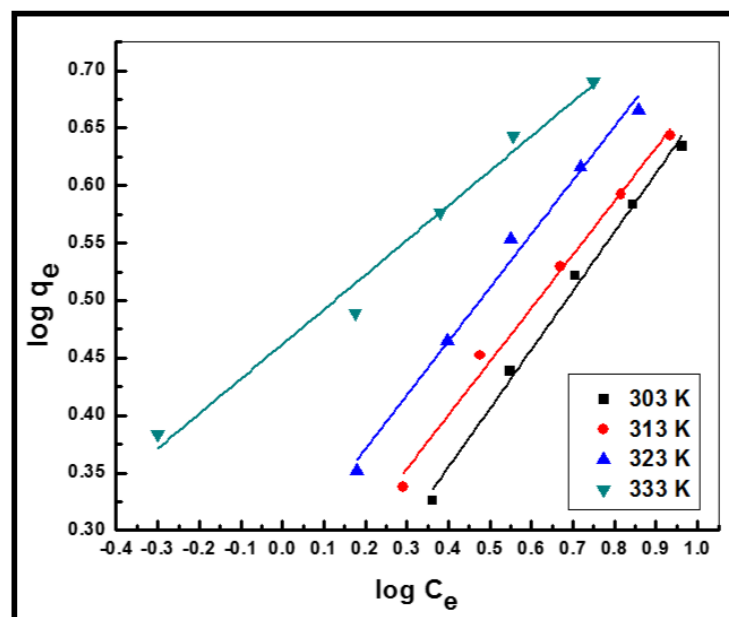
Table 8.5 Langmuir and Freundlich isotherm parameters for linear analysis and non-linear analysis by Microcal origin for adsorption of nickel from aqueous solution on nano-cupric oxide

Analysis	Linear								
Isotherm	**Langmuir Parameters**				**Freundlich Parameters**				
Temperature (K)		**303**	**313**	**323**	**333**		**303**	**313**	**323**	**333**
Constants	Q^o (mg/)	5.65	6.21	6.51	6.57	K_F (mg/g (L/mg)$^{1/n}$)	1.41	1.64	1.89	2.89
	b (L/mg)	0.20	0.27	0.34	0.99	**n**	1.95	2.15	2.14	3.31
Coefficient of determination (R^2)		0.999	0.995	0.999	0.981		0.992	0.989	0.987	0.978

8.2.3.2 Non-linear analysis of adsorption isotherm

Non-linear analysis was performed by altering in-built functions namely Langmuir EXT 1, and Freundlich EXT of origin for Langmuir and Freundlich equations, respectively (Figure 8.14 and 8.15). In addition, customized isotherm function was also used in origin where initial parameter was taken as numerically one. On curve fitting, the in-built functions for both the models exhibited well agreement between the experimental data and data predicted by the model. The customised user defined functions, in contrast showed difference between the experimental and data predicted by the model for Langmuir isotherm (Figure 8.16), whereas, it well described the Freundlich isotherm model (Figure 8.17). Hence, non-linear method predicted Freundlich to be the more suitable isotherm (Table 8.6 and 8.7) in contrast to that of linear approach that suggested Langmuir isotherm model to explain the equilibrium data.
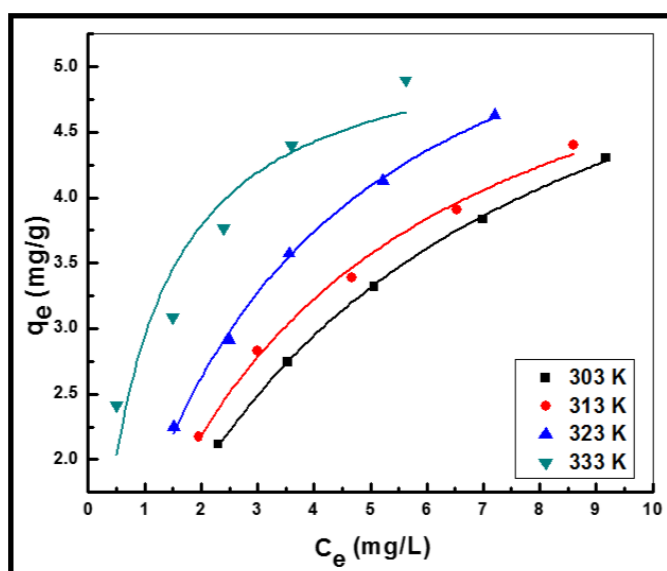

Figure 8.14 Non-linear Langmuir isotherm plot of nickel removal on nano-cupric oxide obtained by in-built Microcal origin function (symbols represent the experimental data and lines represent the data estimated by the model)

Figure 8.15 Non-linear Freundlich isotherm plot of nickel removal on nano-cupric oxide obtained by in-built Microcal origin function (symbols represent the experimental data and lines represent the data estimated by the model)
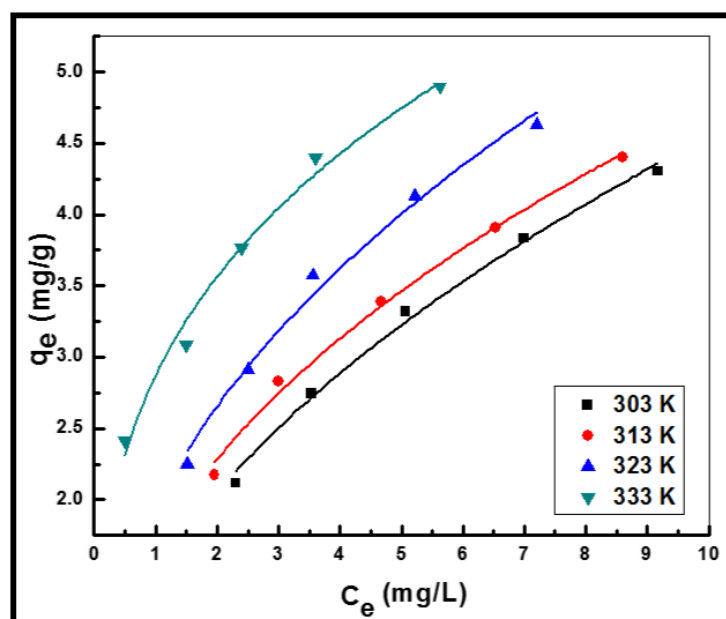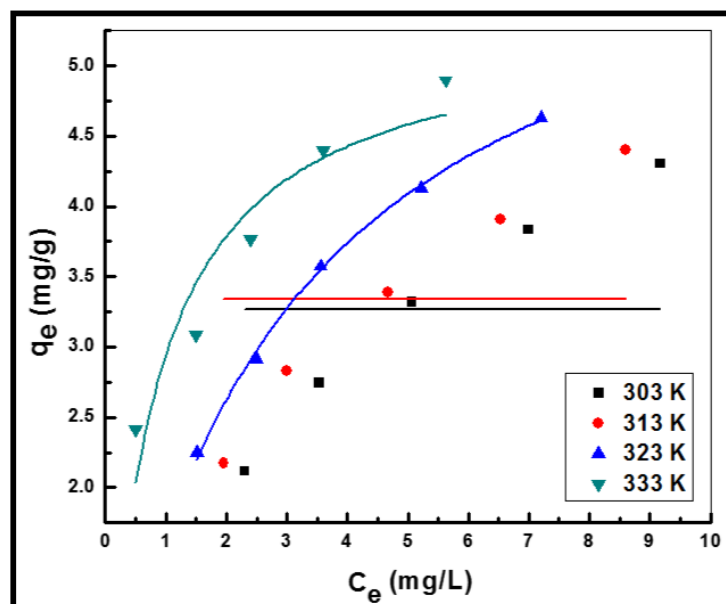

Figure 8.16 Non-linear Langmuir isotherm plot of nickel removal on nano-cupric oxide obtained by customized Microcal origin function (symbols represent the experimental data and lines represent the data estimated by the model)

Figure 8.17. Non-linear Freundlich isotherm plot of nickel removal on nano-cupric oxide obtained by customized Microcal origin function (symbols represent the experimental data and lines represent the data estimated by the model)
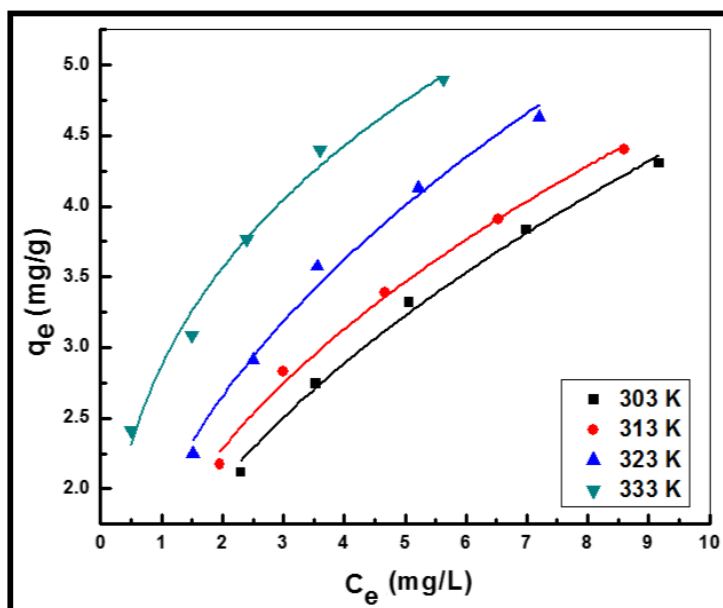
On the basis of coefficient of determination (R^2) values of both linear as well as non-linear analysis, linear approach displayed higher values than that of non-linear approach. Thus, on the basis of high values of coefficient of determination, linear analysis was preferred on non-linear analysis and Langmuir isotherm model was considered for the interpretation of adsorption equilibrium data.

Table 8.6 Langmuir and Freundlich isotherm parameters for non-linear analysis obtained by in-built Microcal origin functions for adsorption of nickel from aqueous solution on nano-cupric oxide

Analysis	Non-linear									
Isotherm	Langmuir Parameters					Freundlich Parameters				
Temperature (K)		303	313	323	333		303	313	323	333
Constants	Q^o (mg/)	5.32	6.18	6.51	6.57	K_F (mg/g (L/mg)$^{1/n}$)	1.45	1.67	1.95	2.87
	b (L/mg)	0.20	0.27	0.34	1.23	n	0.49	0.45	0.44	0.31
Coefficient of determination (R^2)		0.999	0.993	0.997	0.867		0.993	0.993	0.986	0.981

Table 8.7 Langmuir and Freundlich isotherm parameters for non-linear analysis obtained by customized Microcal origin functions for adsorption of nickel from aqueous solution on nano-cupric oxide

Analysis	Customized									
Isotherm	Langmuir Parameters					Freundlich Parameters				
Temperature (K)		303	313	323	333		303	313	323	333
Constants	Q^o (mg/)	3.26	3.34	6.51	5.32	K_F (mg/g (L/mg)$^{1/n}$)	1.45	1.67	1.94	2.87
	b (L/mg)	6.6E+44	2.7E+45	0.33	1.24	n	2.02	2.21	2.23	3.21
Coefficient of determination (R^2)		-0.33	-0.33	0.997	0.867		0.993	0.993	0.986	0.981

8.2.4 Adsorption kinetic modeling

In order to investigate the rate governing step of adsorption, the mechanism of interaction of adsorbent and adsorbate and rate of metal uptake, the adsorption data has been fitted to kinetic models, namely pseudo-first-order, pseudo-second-order and intra-particle diffusion models [Uma et al. 2013]. In addition, linear and non-linear analysis of the adsorption data has been carried out in order to achieve the best fit kinetic model.

The pseudo-first-order kinetic model has been widely used to predict the sorption kinetics and can be expressed by the following linear and non-linear equations [Hodaifa et al., 2013]:

$$dq/dt = k_1 (q_e - q_t) \tag{8.6}$$

$$ln (q_e - q_t) = ln\, q_e - k_1 t \tag{8.7}$$

$$q_t = q_e (1 - exp (-k_1 t)) \tag{8.8}$$

where, $k_1 (min^{-1})$ is the first order rate constant, q_e and q_t are the amount of adsorbate species adsorbed on adsorbent at equilibrium and at any time, t, respectively.

Pseudo-second order model is based on the assumption that the rate limiting step is chemi-sorption in nature. The model is represented in the form of following linear and non-linear equations [Ho and McKay, 1998]:

$$dq/dt = k_2 (q_e - q_t)^2 \tag{8.9}$$

$$q_t = k_2 q_e^2\, t\, /\, 1 + k_2\, q_e\, t \tag{8.10}$$

where, k_2(g mg^{-1} min^{-1}) is the rate constant for pseudo-second-order model equation.

8.2.4.1 Linear analysis of adsorption kinetics

For linear analysis, the kinetic parameters viz., k_1 and q_e values for pseudo-first-order model (Lagergren model), were determined from the slope and intercept of the plot of log (q_e-q_t) vs. t, respectively as shown in Figure 8.18. For, pseudo-second-order kinetic parameters the plot of t/q_t vs. t for the model yielded a straight line from which k_2 and the equilibrium adsorption capacity (q_e) were calculated from the intercept and slope of this line, respectively as shown in Figure 8.19.
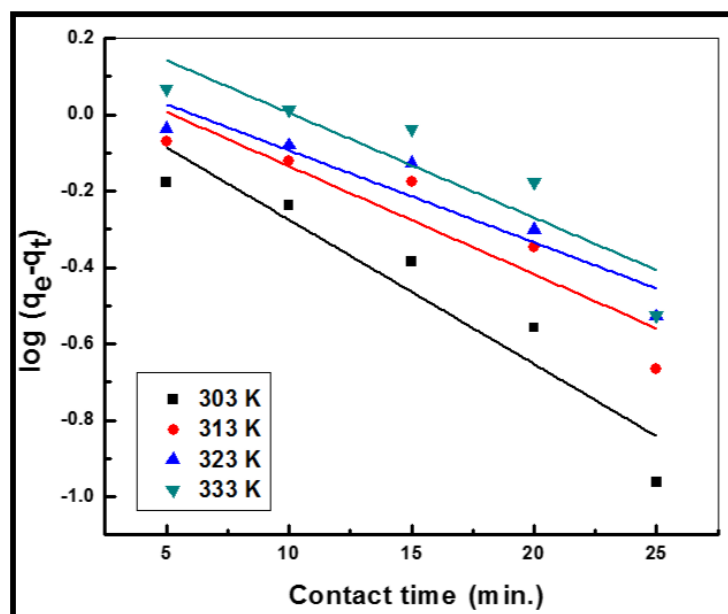

Figure 8.18 Linear pseudo-first order plot of nickel removal on nano-cupric oxide (symbols represent the experimental data and straight lines represent the data estimated by the model)

Figure 8.19 Linear pseudo-second order plot of nickel removal on nano-cupric oxide (symbols represent the experimental data and straight lines represent the data estimated by the model)
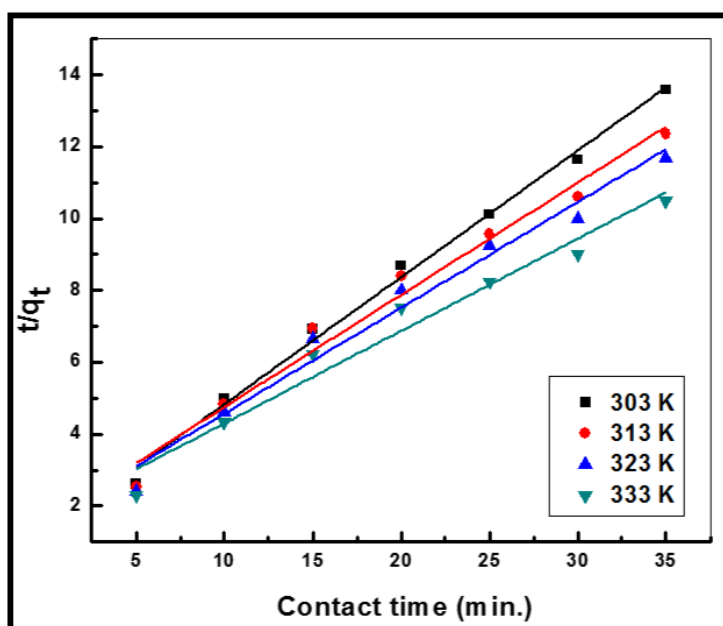
The values of the constants of pseudo-first-order and pseudo-second-order kinetic models, along with their corresponding correlation coefficients were presented in Table 8.8. On comparing the q_e(cal) values with the q_e(exp) values determined by both the models, the values obtained by pseudo-second-order model were very close to q_e(exp) values for all temperatures under study than pseudo-first-order model. The value of correlation coefficient (R^2) for pseudo-first-order model was also lower as compared to pseudo-second-order kinetics model. Thus, it was inferred from the value of R^2 and closeness of experimental and theoretical adsorption capacity (q_e) that pseudo-second order kinetic model better explained the experimental data on linear analysis.

Table 8.8 Pseudo-first order and pseudo-second order kinetic parameters
for linear analysis and non-linear analysis by Microcal origin for
adsorption of nickel from aqueous solution on nano-cupric oxide

Kinetic model	Pseudo-first order Parameter						
Analysis		Linear			Non-linear		
Temperature (K)	q_e (exp.)	q_e (mg/g)	k_1 (1/min)	R^2 adj.	q_e (mg/g)	k_1 (1/min)	R^2 adj.
303	2.58	1.27	0.08	0.927	2.42	0.25	0.494
313	2.83	1.40	0.05	0.759	-1.4E+04	-7.5E-06	-5.997
323	2.99	1.41	0.07	0.875	-1.1E+04	-9.6E-06	-5.405
333	3.33	1.91	0.06	0.899	-1.4E+04	-8.3E-06	-3.179
Kinetic model	Pseudo-second order Parameter						
Analysis		Linear			Non-linear		
Temperature (K)	q_e (exp.)	q_e (mg/g)	k_2 (g.mg^{-1} min^{-1})	R^2 adj.	q_e (mg/g)	k_2 (g.mg^{-1} min^{-1})	R^2 adj.
303	2.58	2.84	0.09	0.993	2.69	0.39	0.789
313	2.83	3.21	0.06	0.977	2.95	0.29	0.685
323	2.99	3.40	0.05	0.972	3.11	0.29	0.659
333	3.33	3.89	0.04	0.961	3.57	0.22	0.697

8.2.4.2 Non-linear analysis of adsorption kinetics

In built functions of Microcal origin namely Langmuir EXT 1 and BoxLucas 1
were incorporated for non-linear analysis of adsorption data for pseudo-first order and

pseudo-second order kinetic equations respectively (Figure 8.20 and 8.21). Customized

user defined isotherm function was also used in which initial parameter was taken as

numerically one similar to that of the non-linear analysis of isotherm (Figure 8.22 and
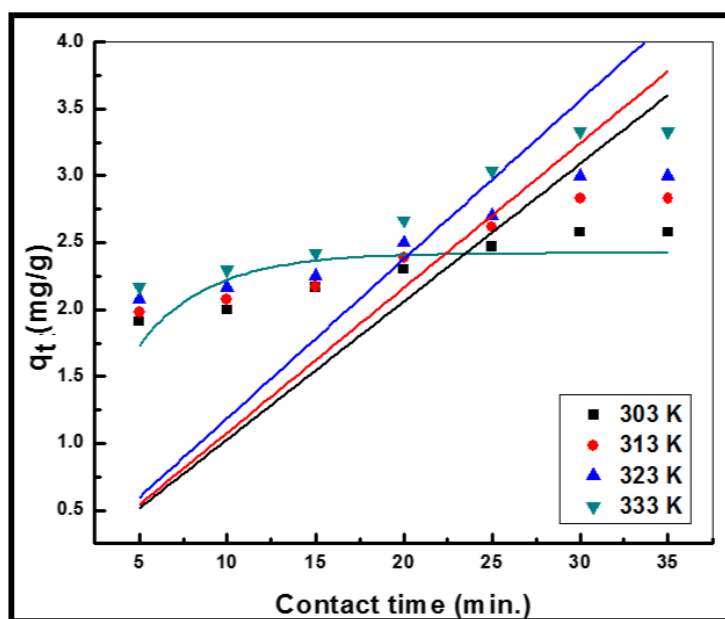
8.23).

Figure 8.20 Non-linear pseudo-first order plot of nickel removal on nano-cupric oxide obtained by customized Microcal origin function (symbols represent the experimental data and lines represent the data estimated by the model)

Figure 8.21 Non-linear pseudo-second order plot of nickel removal on nano-cupric oxide obtained by in-built Microcal origin function (symbols represent the experimental data and lines represent the data estimated by the model)

Figure 8.22 Non-linear pseudo-first order plot of nickel removal on nano-cupric oxide obtained by customized Microcal origin function (symbols represent the experimental data and lines represent the data estimated by the model)
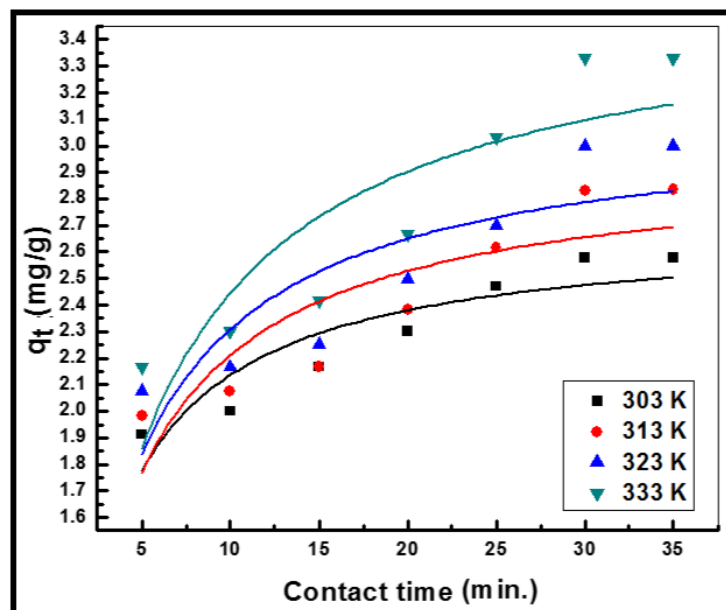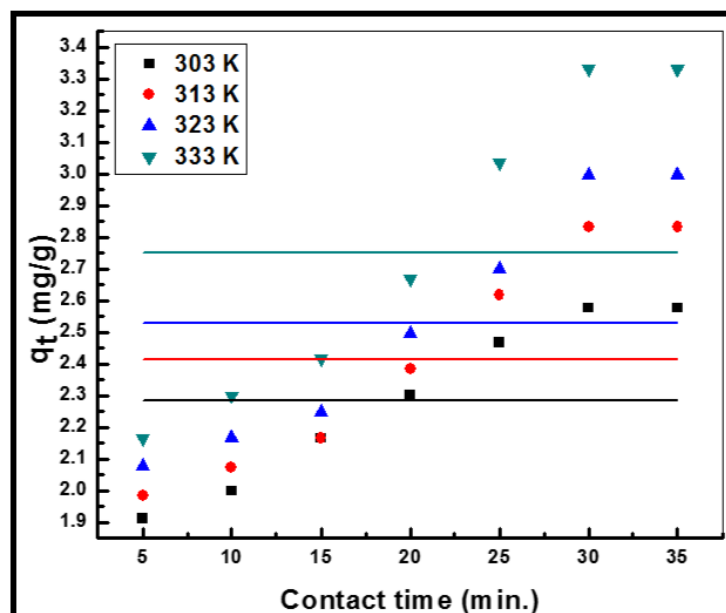
Figure 8.23 Non-linear pseudo-second order plot of nickel removal on nano- cupric oxide obtained by customized Microcal origin function (symbols represent the experimental data and lines represent the data estimated by the model)
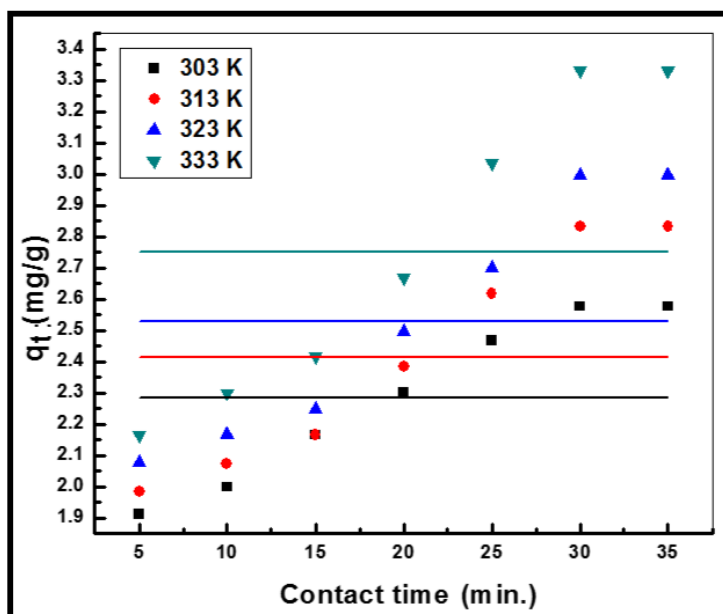
Non-linear analysis through both the in-built functions as well as customized user defined functions depicted that there lies a significant difference between the experimental data and the data estimated by the models (Tables 8.8 and 8.9). Thus, among predictions made by both the linear as well as non-linear approaches, linear approach of kinetic analysis having high R^2 values was preferred on non-linear approach for determination of kinetic parameters.

Table 8.9 Pseudo-first order and pseudo-second order kinetic parameters for linear analysis and non-linear analysis by customized Microcal origin for adsorption of nickel from aqueous solution on nano-cupric oxide

Analysis	Customized							
Kinetic model		Pseudo-first order Parameter				Pseudo-second order Parameter		
Temperature (K)	q_e (exp.)	q_e (mg/g)	k_1 (1/min)	R^2 adj.	q_e (mg/g)	k_1 (1/min)	R^2 adj.
303	2.58	2.29	1.5E+09	-0.2	4.4E+45	2.29	-0.2
313	2.83	2.41	2.9E+09	-0.2	5.0E+43	2.41	-0.2
323	2.99	2.53	5.9E+10	-0.2	-8.4E+44	2.53	-0.2
333	3.33	2.75	9.7E+09	-0.2	-9.9E+41	2.75	-0.2

8.2.4.3 Intra-particle diffusion

Later on, data was fitted to the intra-particle diffusion model for investigating any possibility of diffusion, which is based on diffusive mass transfer where the adsorption rate expressed in terms of the square root of time (t) [Weber and Morris, 1963]:

$$q_t = K_{id}\, t^{0.5} + C \qquad\qquad (8.11)$$

The plot of q_t vs. the square root of time at different temperatures has been shown in Figure 8.24 A. The values of intra-particle diffusion rate constant, K_{id} (mg g^{-1}min$^{-1/2}$) and film thickness, C (mg g^{-1}) calculated from the intercept and slope of the plot, respectively

along with their correlation coefficients have been presented in Table 8.10. Value of C gives an idea about the boundary layer thickness. Larger the value of C, greater will be the boundary layer effect on the adsorption process.
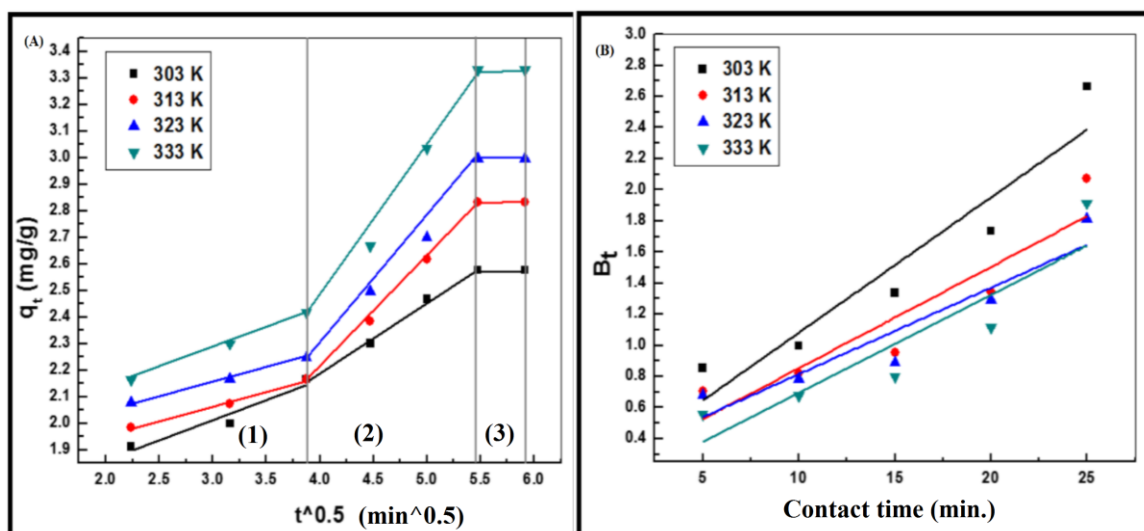

Figure 8.24 A) Intra-particle diffusion plot for removal of nickel from aqueous solution on nano-cupric oxide. B) Boyd model plot for removal of nickel from aqueous solution on nano-cupric oxide.

The intra-particle diffusion plot exhibited multi-linearity and has been demarcated into three regions being marked as 1, 2 and 3 where each domain has its own significance. The regions 1 and 2 represent film diffusion and intra-particle diffusion respectively, whereas region 3 represent the interior surface of adsorbent where adsorption occurred. For intra-particle diffusion to be the rate-controlling step in the process, the plots must pass through the origin but in this case none of the three plots passed through the origin. Thus, the probability of intra-particle diffusion as rate-

controlling step was ruled out but high determination coefficient indicated its significant

role during initial stages of the process [Mohanty et al., 2005; Stankovic´ et al., 2016].

Table 8.10 Intra-particle diffusion constant values for removal of nickel from aqueous
solution on nano-cupric oxide

S. No.	Concentration (mg/L)	K_{id} (mg/g min$^{1/2}$)	C (mg/L)	R^2
1	303	0.20	1.41	0.966
2	313	0.26	1.28	0.919
3	323	0.28	1.31	0.906
4	333	0.36	1.21	0.910

8.2.4.2 Boyd model

In order to explore the probable mechanism of adsorption further, the Boyd model

was applied on the kinetic data. This model distinguishes the film diffusion (boundary

layer) and pore diffusion (diffusion inside adsorbent pores). It can be expressed as

follows [Hu et al., 2011]:

$$B_t = -0.4977 - ln\ (1 - F) \tag{8.12}$$

where, F is the fraction of adsorbed adsorbate at any time t (min). B_t was plotted against t

and in present case, the line (Figure 8.24 B) did not pass through origin. It indicated that adsorption has been governed by boundary layer diffusion mechanism.

8.2.5 Adsorption thermodynamic study

8.2.5.1 Effect of temperature

The influence of temperature on the removal of Ni(II) has been investigated at different temperatures ranging from 303 to 333 K and at various concentrations pre-defined for the experimentation. It was observed that percent removal increased with the rise in temperature which advocated the endothermic nature of the adsorption process (Figure 8.25).
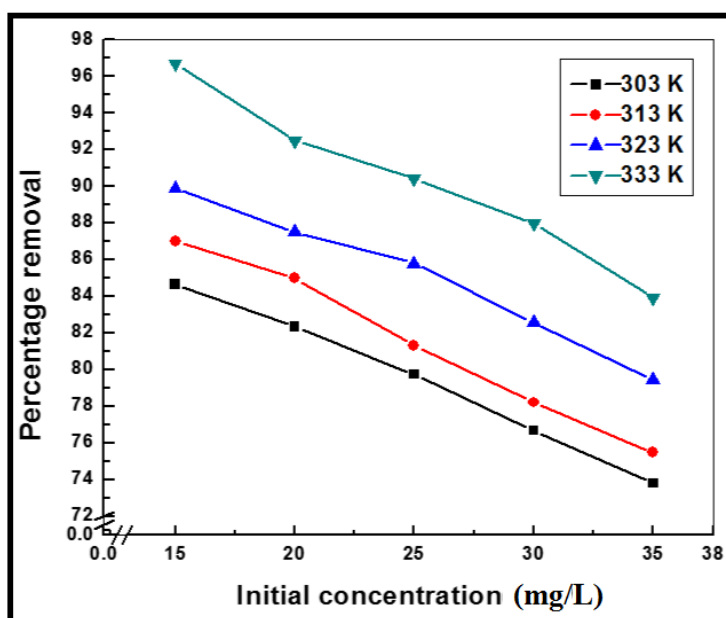

Figure 8.25 Effect of temperature on removal of nickel from aqueous solutions on nano-cupric oxide

This probable reason behind this could be increase in active sites on the surface of adsorbent with increase in temperature that led to increased interaction of metal ions with active sites resulting into increased metal ion removal [Chen et al., 2011].

8.2.5.2 Thermodynamic parameters

The feasibility and spontaneity of the process was explored by thermodynamic parameters such as changes in standard free energy ($\Delta G°$), enthalpy ($\Delta H°$), and entropy ($\Delta S°$) and were evaluated from Langmuir adsorption. The following equations have been used for their estimation [Salvestrini et al., 2014; Brown et al., 2009; Elkady et al., 2011]:

$$\Delta G^{o} = - RT \ln K_L \tag{8.13}$$

$$\ln K_L = \Delta S°/R - \Delta H°/RT \tag{8.14}$$

where, $\Delta G°$ is the Gibbs free energy change, Langmuir constant b is considered as thermodynamic equilibrium constant; K_L (L mol^{-1}), R is universal gas constant (8.314 J•mol^{-1}•K^{-1}), and T is the absolute temperature in Kelvin. Subsequently, the values of $\Delta H°$ and $\Delta S°$ were also determined from the slope and intercept of the plot of ln K_L vs. 1/T, respectively. The values of $\Delta G°$, $\Delta H°$ and $\Delta S°$ calculated at different temperatures have been tabulated in Table 8.11.

Table 8.11 Thermodynamic parameters for adsorption of nickel from
aqueous solution on nano-cupric oxide

S. No.	Temperature (K)	$\Delta G°$ (kJ mol^{-1})	$\Delta H°$ (kJ mol^{-1})	$\Delta S°$ (J mol^{-1}K^{-1})
1	303	-23.94	41.41	213.4
2	313	-25.48		
3	323	-26.88		
4	333	-30.71		

The negative $\Delta G°$ values affirm the feasibility of the adsorption process as well as the spontaneous nature of adsorption that do not require any external source of energy for its occurrence. Further, the increase in negative value at higher temperature manifested that the spontaneity of adsorption process increased with rise in temperature. In case of physi-sorption, the change of standard free energy varies in the range of -20 to 0 kJ mol^{-1} while for involvement of chemi-sorption, standard free energy varies in the range -80 and -400 kJ mol^{-1} [Avila et al., 2014]. Furthermore, the ($\Delta H°$) values were also found to be very low and positive (41.41 kJ mol^{-1}) which indicated the physi-sorption of Ni(II) on Cupric oxide nanoparticles which was also evident from various characterizations after adsorption besides exhibiting endothermic nature [Sharma et al., 2010]. The positive value 213.4 kJ mol^{-1} K^{-1} of entropy ($\Delta S°$) suggested good affinity of Ni(II) towards the nanoparticles and showed increased randomness at the solid/solution interface during the adsorption process [Saha et al., 2011].

8.2.5.3 Activation energy

Activation energy is defined as the energy that must be oncome in order for a chemical reaction to occur. Being specific to adsorption processes, it is defined as the minimum energy needed for a specific adsorbate-adsorbent interaction to take place, despite the fact that the process may as of now be thermodynamically achievable. The activation energy (Ea) for the adsorption of an adsorbate ion/molecule onto an adsorbent surface in an adsorption process can be evaluated from experimental measurements of the adsorption rate constant at different temperatures according to the Arrhenius equation as follows:

$$ln\ k_2 = ln\ A - E_a/RT \qquad\qquad (8.15)$$

where, k_2 (g mg^{-1} min^{-1}) represents the rate constant obtained from the pseudo-second order kinetic model, E_a (J mol^{-1}) is the Arrhenius activation energy of adsorption and A is the Arrhenius factor. The values of E_a and A can be obtained from the slope and the intercept from the plot of ln k_2 versus 1/T (Figure 8.26). The activation energy was estimated as -24.01 kJ mol^{-1}.
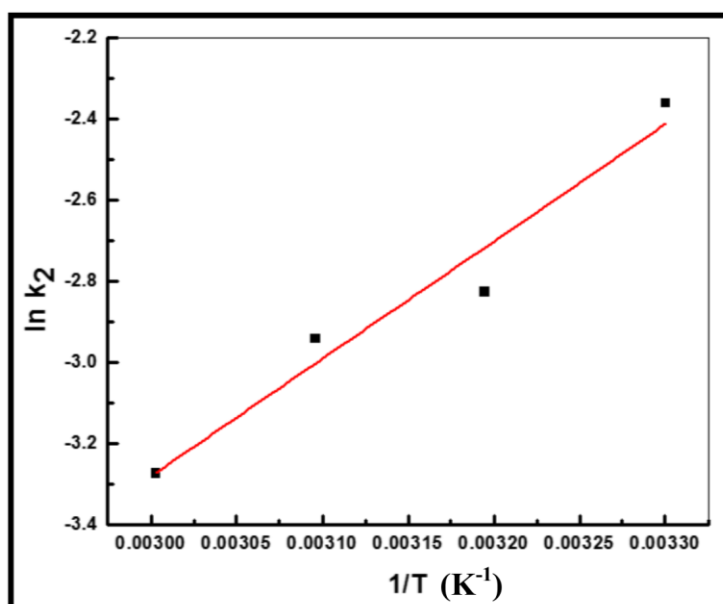
Figure.8.26 Arrhenius plot for removal of nickel from aqueous solution on nano-cupric oxide

8.3 Desorption experiments

The possibility of reuse of exhausted adsorbent has been verified by conducting desorption experiments with three desorbing agents namely HCl (Hydrochloric acid), HNO_3 (Nitric acid) and H_2SO_4 (Sulfuric acid). 0.1N of the aforesaid solutions were prepared and used to desorb the adsorbed nickel ions from the adsorbent and have shown desorption efficiencies as 79.85 %, 89.51 % and 98.68 % respectively. Among all the solutions, maximum desorption efficiency has been exhibited by H_2SO_4 solution and thus it was selected for the desorption purpose. It was found that up to three cycles adsorbent exhibited considerable removal of nickel for reuse as an adsorbent after third cycle the desorption efficiency was reduced (Table 8.12).

Table 8.12 Nickel removal after subsequent regeneration cycle (Initial conc.
=20 mg/L, pH = 7.0, Dose = 6 g/L, Temperature =303 K)

S. No.	Regeneration Cycle	Nickel removal (%)
1	1	98.95
2	2	96.45
3	3	92.37
4	4	79.93

8.4 Conclusions

Cupric oxide (CuO) nanoparticles were synthesized having average particle size in the nano range. The process of adsorptive removal of Ni(II) on CuO nanoparticles from aqueous solutions was modelled via Response Surface Methodological approach. pH of the solution was found to be most influential parameters among various other operational parameters. Under the specified conditions predicted by the model, 100% removal can be achieved at pH 7.0, initial concentration 25mg/L and adsorbent dose 18.8g/L. Increased removal with rise in temperature confirmed the endothermic nature of the adsorption process. Equilibrium was achieved within 30 min of adsorption. The adsorption equilibrium data was best interpreted by Langmuir isotherm model and adsorption kinetics followed pseudo-second order model. Intra-particle diffusion was not the only

rate-controlling step. Boyd model proposed the involvement of film diffusion as a rate controlling step in the process. Furthermore, linear method of analysis was most appropriate than non-linear analysis for determination of isotherm and kinetic parameters. The experimental findings concluded that under optimized conditions, Cupric oxide can be used as an effective adsorbent for treatment of industrial effluents containing nickel ions.